

See discussions, stats, and author profiles for this publication at: <https://www.researchgate.net/publication/264234992>

High-Resolution Solid State ^{13}C NMR Studies of Bent-Core Mesogens of Benzene and Thiophene

ARTICLE in THE JOURNAL OF PHYSICAL CHEMISTRY C · JUNE 2014

Impact Factor: 4.77 · DOI: 10.1021/jp504835c

CITATIONS

9

READS

26

6 AUTHORS, INCLUDING:



[E. Varathan](#)

Central Leather Research Institute

16 PUBLICATIONS 46 CITATIONS

SEE PROFILE



[Nitin P Lobo](#)

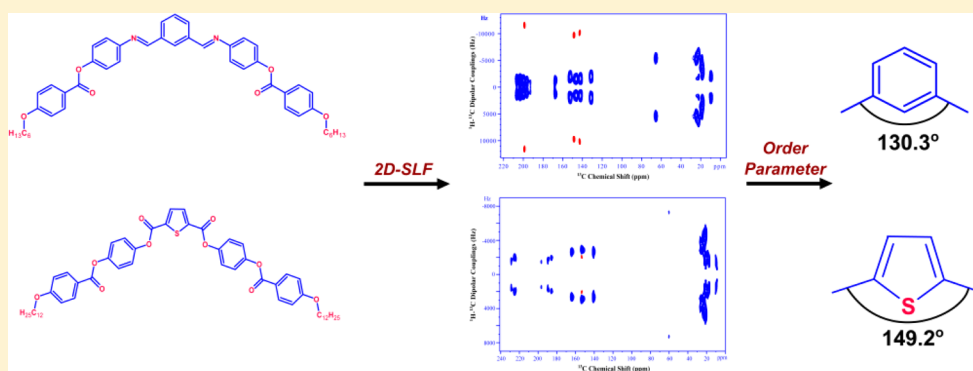
Central Leather Research Institute

19 PUBLICATIONS 76 CITATIONS

SEE PROFILE

High-Resolution Solid State ^{13}C NMR Studies of Bent-Core Mesogens of Benzene and ThiopheneM. Kesava Reddy,[†] E. Varathan,[‡] Nitin P. Lobo,[§] Bibhuti B. Das,[§] T. Narasimhaswamy,[‡] and K. V. Ramanathan^{*,||}[†]Department of Chemistry, S. V. University, Tirupati 517502, India[‡]Chemical Laboratory and Polymer Laboratory, CSIR-Central Leather Research Institute, Adyar, Chennai 600020, India[§]Department of Physics, Indian Institute of Science, Bangalore 560012, India^{||}NMR Research Centre, Indian Institute of Science, Bangalore 560012, India

S Supporting Information



ABSTRACT: Bent-core mesogens are an important class of thermotropic liquid crystals as they exhibit unusual properties as well as morphologies distinctly different from rodlike mesogens. Two bent-core mesogens with differing center rings namely benzene and thiophene are considered and investigated using high-resolution oriented solid state ^{13}C NMR method in their liquid crystalline phases. The mesogens exhibit different phase sequences with the benzene-based mesogen showing a B_1 phase, while the one based on thiophene showing nematic and smectic C phases. The 2-dimensional separated local field (2D-SLF) NMR method was used to obtain the ^{13}C – ^1H dipolar couplings of carbons in the center ring as well as in the side-wing phenyl rings. Couplings, characteristic of the type of the center ring, that also provide orientational information on the molecule in the magnetic field were observed. Together with the dipolar couplings of the side-wing phenyl ring carbons from which the local order parameters of the different subunits of the core could be extracted, the bent angle of the mesogenic molecule could be obtained. Accordingly, for the benzene mesogen in its B_1 phase at 145 °C, the center ring methine ^{13}C – ^1H dipolar couplings were found to be significantly larger (9.5–10.2 kHz) compared to those of the side-wing rings (1.6–2.1 kHz). From the local order parameter values of the center (0.68) as well as the side-wing rings (0.50), a bent-angle of 130.3° for this mesogen was obtained. Interestingly, for the thiophene mesogen in its smectic C phase at 210 °C, the ^{13}C – ^1H dipolar coupling of the center ring methine carbon (2.11 kHz) is smaller than those of the side-wing phenyl ring carbons (2.75–3.00 kHz) which is a consequence of the different structures of the thiophene and the benzene rings. These values correspond to local order parameters of 0.85 for the center thiophene ring and 0.76 for the first side-wing phenyl ring and a bent-angle of 149.2°. Thus, the significant differences in the dipolar couplings and the order parameter values between different parts in the rigid core of the mesogens are a direct consequence of the nature of the center ring and the bent structure of the molecule. The present investigation thus highlights the ability of the ^{13}C 2D-SLF technique to provide the geometry of the bent-core mesogens in a straightforward manner through the measurement of the ^{13}C – ^1H dipolar couplings.

■ INTRODUCTION

Thermotropic liquid crystals based on banana or bent-core have emerged as a distinct class of molecular materials.^{1,2} The insertion of a bend at the center of the core facilitates realization of many molecular materials with unusual mesophase morphologies.^{3–5} The subtle difference between banana and bent-core systems lies on the bent-angle generated

by the respective systems.^{6,7} Typically, a bent angle of around 120° would result in banana mesophases, whereas large bent-angles of about 145° results in conventional calamitic

Received: May 16, 2014

Revised: June 20, 2014

Published: June 20, 2014



mesophases and such mesogens are usually classified as bent-core molecules.^{1–3,8} The variation in bent angle depends on molecular structure and more specifically on the size of the carbocyclic or heterocyclic ring at the center of the molecule.² Consequently, benzene with 1,3-disubstitution results in banana mesogens, while five-membered heterocyclics favor bent-core structures.^{9–11} The mesophases observed from banana mesogens have been classified as distinct compared to conventional calamitics based on miscibility studies.² The mesophases generated by bent-core systems on the other hand are comparable to the conventional calamitic mesophases such as the nematic, smectic A, and smectic C phases. However, special features like the phase biaxiality, helical structures as well as ferro and antiferro electric switching make the bent-core mesogens very interesting.^{2,10–12} Since the bent angle of the core in the mesophase is an important factor that influences mesophase morphologies, the determination of bent angle is pertinent and crucial. Often the bent angle for banana as well as bent-core mesogens is determined from energy minimized structures in gas phase from quantum chemical calculations.¹³ Among the experimental techniques, solid state NMR has emerged as an important tool for estimating the bent-angle of the banana mesogens. For instance, Weissflog et al. used ¹³C chemical shifts in the mesophase for arriving at the bent angle of benzene-based banana mesogens.^{14–17} Dong et al. also employed ¹³C NMR for finding the bent angle of a banana mesogen, exhibiting a nematic phase.^{18,19} In this work, we have employed one- and two-dimensional ¹³C NMR approaches to study a banana and a bent-core mesogen to examine the mesophase morphology and the orientational behavior. For the banana mesogen, benzene is employed as a central core, and for the bent core, the thiophene ring served as the center ring. Mesophase transitions have been obtained and XRD data for the bent-core system has been additionally used to characterize the material. The main focus of the work is on utilizing ¹³C–¹H dipolar couplings for obtaining the orientational order parameters and the bent angle from them.

■ EXPERIMENTAL SECTION

The compounds namely 4,4'-(1*E*,1'*E*)-[1,3-phenylenebis(methan-1-yl-1-ylidene)]bis(azan-1-yl-1-ylidene)bis(4,1-phenylene)bis(4-(hexyloxy)benzoate) (PMBAPH) and bis[4-(4-dodecyloxy) benzoyloxy phenyl] thiophene-2,5-dicarboxylate (BDBPTD) were synthesized by multistep synthetic routes. The experimental procedure and the spectral data are provided in the Supporting Information.

Instrumental Details. FT-IR spectra of the compounds were recorded on ABB BOMEM MB3000 spectrometer using a KBr pellet. ¹H and ¹³C NMR spectra of the compounds in CDCl₃ as a solvent were recorded on a Bruker AV-III 400 MHz instrument at room temperature using tetramethylsilane as an internal standard. The resonance frequencies of ¹H and ¹³C were 400.23 and 100.64 MHz, respectively. The nature of the mesophase and the temperature of occurrence were determined with an Olympus BX50 hot-stage optical polarizing microscope (HOPM) equipped with a Linkam THMS 600 stage with a TMS 94 temperature controller. The photographs were taken using an Olympus C7070 digital camera. Differential scanning calorimetry (DSC) traces were recorded using a DSC Q200 instrument with a heating rate of 10 °C/min in nitrogen atmosphere. The data obtained from second heating and cooling is used for discussion.

Computational Details. Density functional theory (DFT) provides a means for computing a variety of ground-state properties with high accuracy. Calculated structures of organic molecules in the ground-state (*S*₀) with the Becke's three-parameter functional and the Lee–Yang–Parr (B3LYP) functional often provide good agreement with crystal geometries. Thus, the ground state (*S*₀) geometrical optimization of PMBAPH and BDBPTD in gas phase was carried out at the level of B3LYP/6-31G*.^{20,21} The NMR chemical shifts were calculated at the B3LYP/6-311+G(2d,p) level of theory using the gauge invariant atomic orbitals (GIAO) method to circumvent the gauge problem using B3LYP/6-31G(d) geometry.²² Cheeseman recommended the 6-311+G(2d,p) basis set for NMR chemical shifts after scrutiny of various basis sets and hence the same was selected for the present study.²³ The scale factor determined for B3LYP/6-311+G(2d,p)//B3LYP/6-31G(d) methodology from the previous study was used for the calculation of ¹³C NMR chemical shifts.²⁴ Accordingly, $d_{\text{scal}} = 0.95d_{\text{calc}} + 0.30$, where d_{calc} and d_{scal} are the calculated and the linearly scaled values of the ¹³C chemical shifts, respectively. The chemical shift values of tetramethylsilane calculated at the same level of theory were used as the reference (182.5 ppm).²⁴ All calculations were carried out with Gaussian 09.²⁵

X-ray Measurements. X-ray diffraction (XRD) was carried out using Cu Kα ($\lambda = 1.54$ Å) radiation from DY 1042-Empyrean XRD with PCS and Pixel system (Diffractometer System-Empyrean, measuring program-focusing mirror, scans axis-gonioKAlpha-1.54060, goniometer radius-240 mm, and modification editor: Panalytical).²⁶

Solid State NMR Measurements. Solid state NMR experiments were carried out on a Bruker AV-III 500 MHz NMR spectrometer. All the static experiments on liquid crystalline samples were performed on a 5 mm double resonance static probe with a horizontal solenoid coil. The proton and carbon resonance frequencies were 500.17 and 125.79 MHz, respectively. The 90° proton pulse width was 4 μs. For cross-polarization, a contact time of $\tau = 3$ ms and 62.5 kHz of rf were used in both carbon and proton channels for the Hartmann–Hahn match condition. Proton decoupling during the ¹³C signal acquisition was done by the SPINAL-64²⁷ pulse sequence with an rf field strength of 30 kHz. The one-dimensional (1D) spectrum was acquired with 512 scans with a recycle delay of 10 s between scans to avoid sample heating. For measuring the ¹³C–¹H dipolar couplings of the mesogens in their mesophase, the SAMPI-4 pulse sequence was applied on the oriented sample under static conditions.²⁸ The earlier work describes the application of the pulse sequence to liquid crystalline systems.^{29–31} The technique gives a 2D spectrum which correlates the proton-carbon dipolar oscillation frequencies along the *F*₁ dimension on the basis of carbon chemical shifts along the *F*₂ dimension. The SAMPI-4 experimental parameters chosen for the PMBAPH/BDBPTD were as follows: contact time, $\tau = 3$ ms/3 ms, number of data *t*₁ points = 128/100, number of data *t*₂ points = 512/512, number of scans = 96/64, relaxation delay = 12s/16s, and 90° pulse width = 4 μs. A shifted sine bell window function was applied to the time domain data and the spectrum was processed in the phase sensitive mode.

■ RESULTS AND DISCUSSION

The planar as well as energy-optimized structures of PMBAPH and BDBPTD mesogens are shown in Figure 1. The synthesis

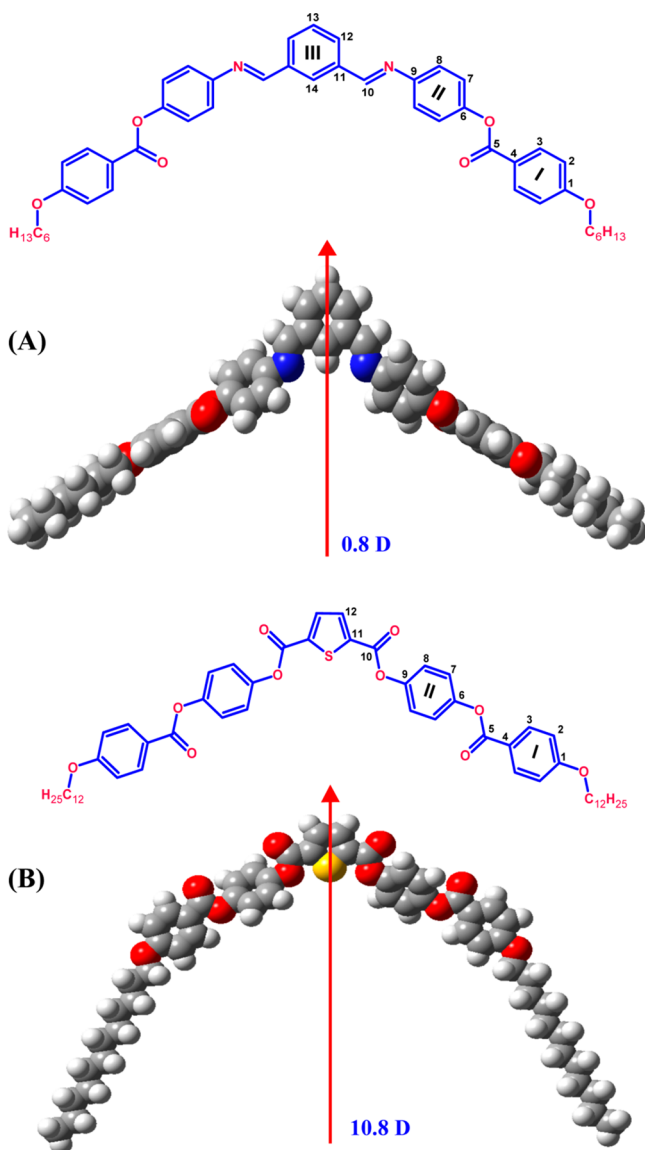


Figure 1. Molecular structures, energy-optimized space-filled models, and direction of dipole moment of (A) PMBAPH and (B) BDBPTD.

and mesophase property of PMBAPH was first reported by Bedel et al.³² The synthetic strategy employed in the present work is shown in the Supporting Information, and it differs with the earlier reported work in the final step. The PMBAPH mesogen is a five phenyl ring-based symmetrical molecule with a central phenyl ring linked to side wings at the 1,3-position. The side wing is constructed with two phenyl ring core linked by the ester unit, and these wings are joined to the center ring by the imine group. The hexyloxy chain is attached to the para position of the ring-I which serves as the terminal unit. For BDBPTD, thiophene is placed at the central location with phenyl rings connected by ester group in the side arm to create a bent-core unit. The BDBPTD mesogen is synthetically novel (Supporting Information), and the mesophase characteristics are reported first time. The structural confirmation of PMBAPH and BDBPTD is carried out with FT-IR, solution ^1H and ^{13}C NMR spectroscopy. The mesophase transition temperatures and phase assignment are carried out by HOPM and further confirmed by DSC (Supporting Information). The PMBAPH on cooling from the isotropic melt shows dendritic

growth. On further cooling, the dendritic aggregates transform to a mosaic texture (Supporting Information).^{4,33} The mesophase transitions found from DSC measurements are crystal to B_1 phase at 136.6 °C and B_1 to isotropic phase at 154.7 °C (Supporting Information). The corresponding enthalpy values are 8.68 and 3.83 kcal/mol respectively (Supporting Information). The high enthalpy value of clearing transition is typical of banana mesophases.³ The mesophase data is consistent with the earlier report, where the existence of B_1 mesophase was unequivocally confirmed by X-ray measurements. Thus, the XRD of the PMBAPH in small-angle region shows two reflections whose ratio is found to be 1.22, and at a wide angle, a diffuse scattering indicating absence of in-plane order within the layers. These features support the existence of B_1 mesophase in PMBAPH.³² The dipole moment of PMBAPH was obtained as 0.8 D from DFT of quantum chemical calculations.

The HOPM and DSC studies support dimorphism for bent-core mesogen (BDBPTD) (Supporting Information), and accordingly, it showed peaks in DSC on heating and cooling scans. The DSC scan on heating shows Cr– S_C at 186.5 °C, S_C –N at 251.4 °C, and N–I at 275.2 °C. The mesophase sequence is established from HOPM textures by cooling the sample from the isotropic phase. It exhibits nematic and smectic C phases before crystallization on cooling the isotropic phase (Supporting Information). The mesophase stability (88.7 °C) is found to be good despite the bent-core shape, and the high melting temperature is a direct consequence of high symmetry. Further, the molecular anisotropic polarizability plays a crucial role in altering the transition temperatures. The dipole moment value determined from quantum chemical calculations is 10.8 D for BDBPTD. Such a large dipole moment is a consequence of the C_2 symmetry of the molecule and the presence of the polarizable ester linking units which connect the side wing phenyl rings.

XRD Studies of BDBPTD. Figure 1B shows the energy minimized structure of BDBPTD in which alkoxy terminal chains are shown as extended part of the side arm. However, to account for the floppy state of the chains which extend along the layering direction especially to reduce the steric volume, the following estimate of the molecular length is considered. The length between the two ends of the core is 23.7 Å. The dodecyloxy chain length for each arm is found to be 16.3 Å, and thus the total length of the terminal chains is taken to be 32.6 Å. Hence, adding the core and the terminal chain lengths, the overall molecular length is taken to be ~56 Å. The powder X-ray diffraction at four different temperatures in the smectic C phase is carried out (Table 1), where a sharp intense reflection in the small angle region and a broad and diffuse maximum in the wide angle region are seen. The XRD intensity versus 2θ plot at 215 °C is shown in Figure 2. These features are characteristic of layer ordering typical of smectic phases. The observed “ d ” values are much lower than the molecular length

Table 1. Powder X-ray Diffraction Data of BDBPTD at Different Temperatures

| temp (°C) | d_1 (Å) | d_2 (Å) |
|-----------|-----------|-----------|
| 225 | 38.65 | 4.62 |
| 215 | 38.66 | 4.60 |
| 205 | 38.68 | 4.58 |
| 195 | 38.70 | 4.57 |

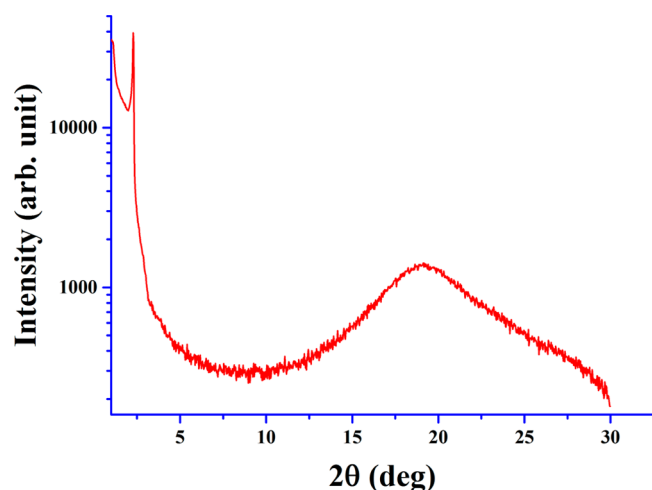


Figure 2. High-resolution X-ray powder diffraction pattern for BDBPTD at 215 °C.

(L) of 56 Å obtained above from the energy minimized structure. Hence at 195 °C, the d/L value is 0.69, which suggests that the molecule is tilted within the layer with the tilt angle being 46.3°. This supports the observation of the smectic C phase from HOPM and DSC investigations. The tilt angle is relatively large and is generally observed for samples in which the nematic phase precedes the smectic C phase.²⁹ The VT-XRD profile from 195 to 225 °C indicates that the tilt angle is constant over the thermal range studied, a behavior again consistent with the nematic–smectic C phase sequence.^{34,35}

¹³C NMR Investigations. *¹³C NMR of PMBAPH and BDBPTD in Solution State.* The carbon numbering of PMBAPH is displayed in Figure 1A, while Figure 3B shows the proton decoupled ¹³C NMR spectrum in CDCl₃ at room temperature. The spectral assignment is carried out using

carbon chemical shifts obtained from DFT (Table 2). For the center ring as well as side wings, 14 sharp lines are observed in

Table 2. ¹³C NMR Data of PMBAPH in Solution and Liquid Crystalline State at 145 °C

| C no. | solution (ppm) | DFT (ppm) | 145 °C | | |
|-------|----------------|-----------|----------------------------|-----------|---|
| | | | B ₁ phase (ppm) | AIS (ppm) | ¹³ C– ¹ H dipolar oscillation frequencies (kHz) |
| 1 | 163.5 | 163.3 | 206.3 | 42.8 | 1.25 |
| 2 | 114.3 | 115.5 | 130.9 | 16.6 | 2.01 |
| 3 | 132.2 | 130.1 | 152.1 | 19.9 | 1.91 |
| 4 | 121.4 | 122.2 | 167.2 | 45.8 | 1.19 |
| 5 | 165.0 | 163.2 | 192.0 | 27.0 | 0.95 |
| 6 | 149.4 | 149.4 | 202.4 | 53.3 | 1.22 |
| 7 | 121.8 | 123.5 | 141.7 | 19.9 | 1.61 |
| 8 | 122.4 | 126.0 | 146.4 | 24.0 | 1.57 |
| 9 | 149.1 | 149.1 | 199.5 | 50.1 | 1.16 |
| 10 | 159.4 | 155.7 | 199.6 | 40.2 | 11.66 |
| 11 | 136.7 | 138.9 | 195.9 | 59.2 | 1.07 |
| 12 | 131.2 | 133.1 | 142.6 | 11.4 | 10.22 |
| 13 | 129.2 | 126.9 | 148.4 | 19.2 | 9.79 |
| 14 | 129.3 | 125.5 | 148.4 | 19.1 | 9.79 |

the 114–165 ppm range. Since PMBAPH is a symmetric molecule with two phenyl rings in the wing and one phenyl ring at the center, seven methine carbon signals are expected, which are observed in the spectrum. Among them, four intense lines in the range of 114–133 ppm are assigned to phenyl ring methine carbons of the side wing. The methine carbons of the center ring and imine carbons showed comparable intensity. The ester carbonyl carbon is observed at 165 ppm, and the characteristic imine carbon is noticed at 159.4 ppm. Among the terminal hexyloxy chain carbons, the OCH₂ (68.3 ppm) and methyl carbon (14.0 ppm) are distinctly seen, while other

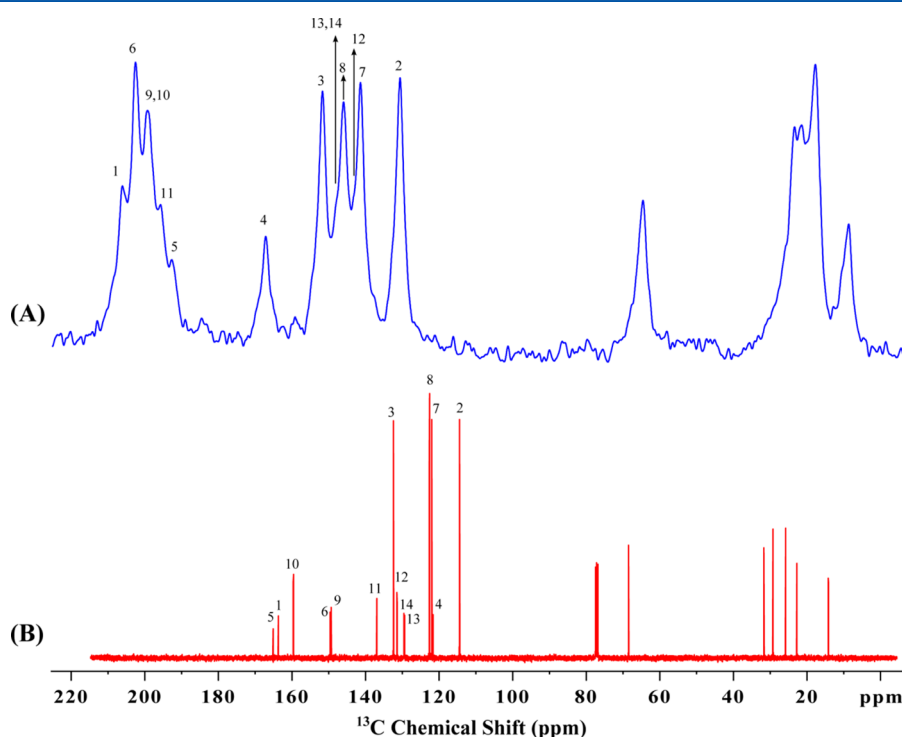


Figure 3. ¹³C NMR spectra of PMBAPH in a (A) liquid crystalline state at 145 °C and a (B) solution state at room temperature.

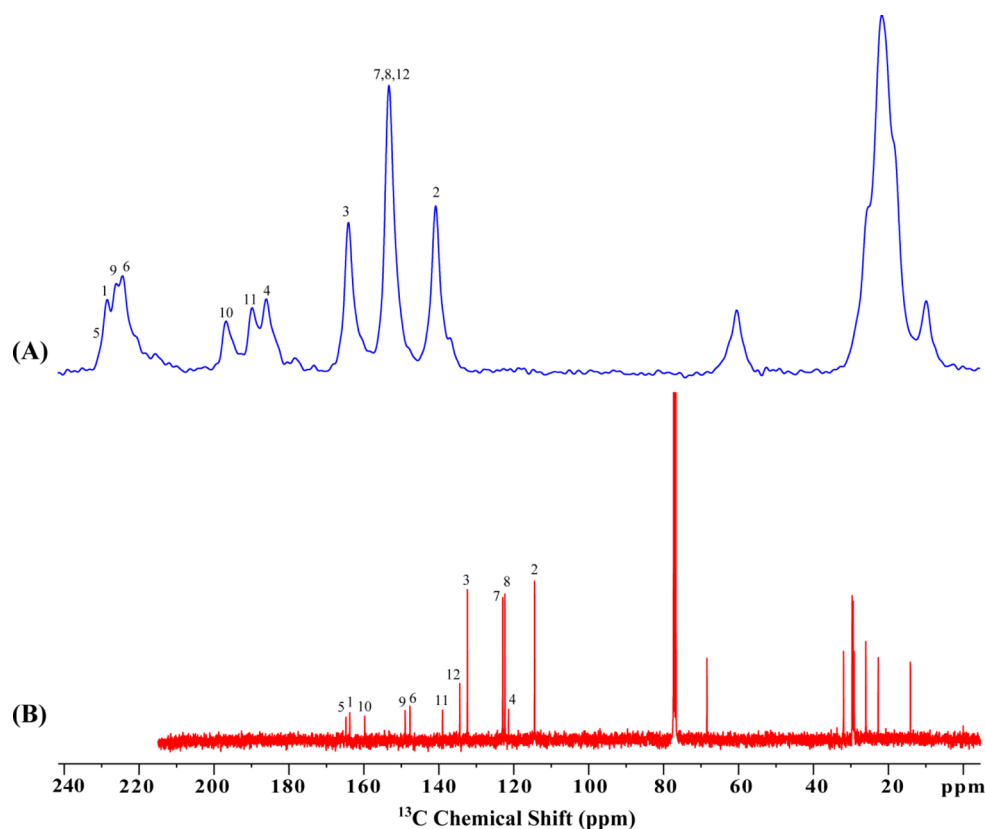


Figure 4. ^{13}C NMR spectra of BDBPTD in (A) liquid crystalline state at 210 $^{\circ}\text{C}$ and (B) solution state at room temperature.

Table 3. ^{13}C NMR Data of BDBPTD in Solution and Liquid Crystalline States at 210 and 230 $^{\circ}\text{C}$

| C no. | solution (ppm) | DFT (ppm) | 210 $^{\circ}\text{C}$ | | | 230 $^{\circ}\text{C}$ | | |
|-------|----------------|-----------|------------------------|-----------|--|------------------------|-----------|--|
| | | | smectic C phase (ppm) | AIS (ppm) | ^{13}C – ^1H dipolar oscillation frequencies (kHz) | smectic C phase (ppm) | AIS (ppm) | ^{13}C – ^1H dipolar oscillation frequencies (kHz) |
| 1 | 163.7 | 161.2 | 228.7 | 65.0 | 1.64 | 224.9 | 61.2 | 1.53 |
| 2 | 114.4 | 117.2 | 140.5 | 26.1 | 2.86 | 139.5 | 25.1 | 2.75 |
| 3 | 132.3 | 134.0 | 163.8 | 31.5 | 2.79 | 162.5 | 30.2 | 2.64 |
| 4 | 121.3 | 124.4 | 185.6 | 64.3 | 1.79 | 184.7 | 63.4 | 1.67 |
| 5 | 164.8 | 162.5 | 229.0 | 64.2 | 0.93 | 227.1 | 62.3 | 0.70 |
| 6 | 147.7 | 148.1 | 224.7 | 77.0 | 1.76 | 218.1 | 70.4 | 1.55 |
| 7 | 122.9 | 122.4 | 153.0 | 30.1 | 3.02 | 151.7 | 28.8 | 2.89 |
| 8 | 122.3 | 121.2 | 153.0 | 30.7 | 3.02 | 151.7 | 29.4 | 2.89 |
| 9 | 149.0 | 149.3 | 226.1 | 77.1 | 1.84 | 221.7 | 72.7 | 1.66 |
| 10 | 159.7 | 157.5 | 196.6 | 36.9 | 1.29 | 194.7 | 35.0 | 1.22 |
| 11 | 139.0 | 143.7 | 189.7 | 50.7 | 1.61 | 187.0 | 48.0 | 1.50 |
| 12 | 134.4 | 133.1 | 153.0 | 18.6 | 2.11 | 152.5 | 18.1 | 1.99 |

methylene carbons are observed in the range of 22–32 ppm. The proton decoupled ^{13}C NMR spectrum of BDBPTD shows 12 lines in the range of 14–165 ppm (Figure 4B), indicating the C_2 symmetry of the molecule. As before, the assignment of the phenyl as well as the thiophene carbons is accomplished by making use of ^{13}C chemical shifts computed from DFT, and the results are displayed in Table 3.

^{13}C NMR Studies of PMBAPH in the B_1 Phase. *1D* ^{13}C NMR. The ^{13}C NMR spectrum of a static sample of PMBAPH was recorded, while cooling the sample from the isotropic melt. Figure 3A shows the spectrum at 145 $^{\circ}\text{C}$ in B_1 phase. The peaks observed in the range of 130–210 ppm arise from the phenyl carbons as well as from carbons in the linking units, whereas the peaks from the terminal chain appear in the range of 9.0–65.5 ppm. Due to the alignment of the molecule in the

magnetic field, the chemical shifts of the core unit carbons showed an increase in contrast to values in solution, while the terminal chain carbons showed marginal decrease.^{36,37} The spectrum in the region 130–155 ppm shows four intense peaks which are due to phenyl ring CH carbons of the mesogen. In the side phenyl rings, the ortho as well the meta carbons become equivalent due to π -flips about the para axis and a single peak is expected for each of them.^{38,39} In the region 195–210 ppm as many as five closely spaced signals are noticed. A peak at 167.2 ppm is distinctly seen and is assigned to the C4 carbon. The assignment of the carbons in the side arm phenyl rings could be carried out by comparison with similar mesogens for which static ^{13}C NMR data is available. For instance, ring-I is structurally comparable with 4-hexyloxy benzoic acid,⁴⁰ whereas ring-II is part of the mesogens for

which ^{13}C NMR studies are recently reported.⁴¹ The chemical shift assignment is additionally aided by the 2D SAMPI-4 spectral data, which is described in the next section. It may be mentioned that the chemical shifts of the aligned mesogen did not exhibit temperature-dependent changes in the range from 142 to 152 °C, a behavior that is in contrast to calamitic mesogens, where lowering the temperature results in increase of the alignment induced chemical shifts (AIS) due to increase in the orientational order parameter. This has been observed earlier by other researchers who also find that aligning the banana mesogens in the magnetic field is difficult, and if they align, the temperature-dependent variations of the chemical shifts are not noticeable.^{42–44}

2D SAMPI-4. The 2D SAMPI-4 spectrum of PMBAPH is shown in Figure 5, which shows intense and well-resolved

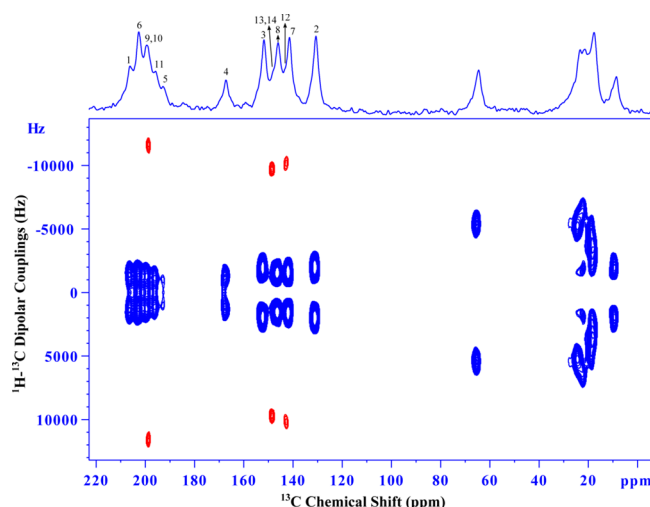


Figure 5. 2D SLF NMR spectrum of PMBAPH in B₁ phase at 145 °C. Red contours denote center phenyl ring methine and methine carbons.

contours. The resolution in the 2D spectrum is much higher than in the 1D spectrum. For example, in the terminal hexyloxy region, in contrast to the 1D spectrum, many carbon contours are resolved due to the differing dipolar couplings at the different carbon sites. A remarkable feature of the 2D spectrum is the clear separation of three contours in the chemical shift range of 130–210 ppm with large dipolar coupling values between 9 and 12 kHz. Among these, the contour with a dipolar coupling of 11.6 kHz is assigned to azomethine carbon appearing around 199.6 ppm. The center phenyl ring methine carbons are assigned to peaks between 142 and 149 ppm with dipolar couplings in the range of 10 kHz. Peaks corresponding to relatively low dipolar couplings (1.6–2.0 kHz) appearing in the range of 130–153 ppm are attributed to side arm phenyl rings, which are expected to show four contours as noticed in the spectrum. The peaks appearing in the range of 165–210 ppm whose ^{13}C – ^1H dipolar couplings are less than 1.3 kHz are assigned to quaternary carbons of phenyl rings and ester carbonyl. Table 2 lists the ^{13}C – ^1H dipolar couplings as well as alignment-induced chemical shifts for all the core unit carbons of PMBAPH mesogen. A significantly large difference between the dipolar couplings of the center phenyl ring and the side-wing phenyl rings is the result of the remarkably different orientations of these units with respect to the orienting axis, as depicted in Figure 6A.^{15–19} The dipolar couplings can be used

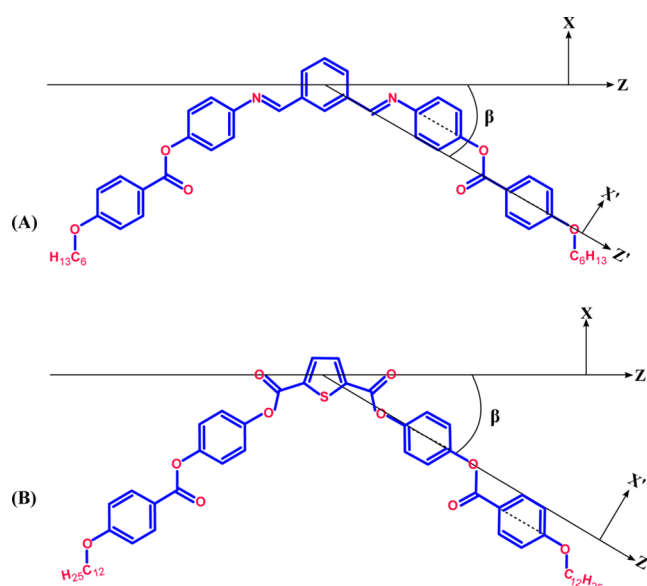


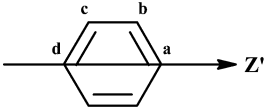
Figure 6. Models depicting molecular frames of (A) PMBAPH and (B) BDBPTD.

to calculate the orientational order parameters of center as well as side-wing phenyl rings using the following relation:^{36,45}

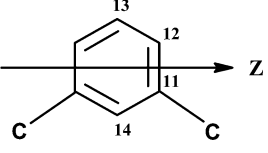
$$D_{\text{CH}} = K \left\{ \frac{1}{2} (3 \cos^2 \theta_z - 1) S'_{zz} + \frac{1}{2} (\cos^2 \theta_x - \cos^2 \theta_y) (S'_{xx} - S'_{yy}) \right\} \quad (1)$$

where $K = -h\gamma_C\gamma_H/4\pi^2r_{\text{CH}}^3$, in which γ_C and γ_H are gyromagnetic ratios of carbon and hydrogen nuclei, respectively. The angles θ_x , θ_y , and θ_z are those between the internuclear vector, r_{CH} , and coordinate axes. For the side-wing phenyl rings, the C_2 axis is taken as the z' axis, the x' axis is in the plane of the rings, while the y' axis is perpendicular to the plane. Whereas for center phenyl ring (ring-III), we have taken the z axis perpendicular to its para axis direction (axis joining carbons 13 and 14) and x -axis collinear to the para axis of the ring, as shown in Figure 6A. The experiment provides dipolar oscillation frequencies from which the dipolar couplings can be extracted by following the established procedure.^{18,29,31,40,41,46–48} For side-wing phenyl rings, methine carbon experimental dipolar frequency has two coupling components, namely, a coupling between attached ipso proton $D_{\text{C-Hi}}$ and also a coupling to its nonbonded ortho proton $D_{\text{C-Ho}}$. Hence, the final frequency given by $[(D_{\text{C-Hi}})^2 + (D_{\text{C-Ho}})^2]^{1/2}$. The quaternary carbon coupled to two equivalent ortho protons, hence, the dipolar frequency will be $\sqrt{2} \times (D_{\text{C-Ho}})$. Accordingly, for the center phenyl ring, the final measured dipolar frequency for C12 carbon can be expressed as $[(D_{\text{C12-H12}})^2 + (D_{\text{C12-H13}})^2]^{1/2}$ and for C13 carbon dipolar frequency will be $[(D_{\text{C13-H13}})^2 + 2(D_{\text{C13-H12}})^2]^{1/2}$. For C14 carbon we considered coupling only to its attached proton [i.e., $(D_{\text{C14-H14}})$]. It has been necessary to vary the two CCH bond angles slightly around 120° during fitting, in the case of side-wing phenyl rings, because of the uncertainty involved in the position of the H atom as determined by X-ray analysis.⁴⁸ For center phenyl ring, the angle made by C_{13} – H_{13} and C_{14} – H_{14} bonds with respect to the z axis has been equally varied, slightly around 90° to retain the symmetry of the ring, and also the angle between the C_{12} – H_{12} bond and z axis has been varied around 30° to arrive at the best fitting. The two-order

Table 4. Orientational Order Parameter Values of PMBAPH



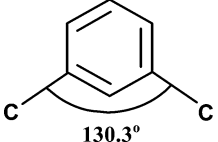
Side-Wing Phenyl Ring



Center Phenyl Ring

| T (°C) | ring | angles | | S'_{zz} | $(S'_{xx} - S'_{yy})$ | calculated dipolar oscillation frequencies (kHz) | | | | RMSD (kHz) |
|--------|------|----------------------------|---------------|-----------|-----------------------|--|-------|------|------|------------|
| | | θ_b | θ_c | | | b | c | a | d | |
| 145 | I | 120.7 | 121.1 | 0.50 | 0.055 | 2.00 | 1.91 | 1.18 | 1.18 | 0.04 |
| | II | 121.9 | 122.0 | 0.50 | 0.043 | 1.65 | 1.63 | 1.17 | 1.18 | 0.04 |
| | ring | θ_{13}, θ_{14} | θ_{12} | S_{zz} | $(S_{xx} - S_{yy})$ | 11 | 12 | 13 | 14 | RMSD |
| | III | 89.7 | 27.2 | 0.68 | 0.166 | — | 10.21 | 9.97 | 9.60 | 0.15 |

Bent Angle



130.3°

parameters, namely, S'_{zz} and $(S'_{xx} - S'_{yy})$ for all the phenyl rings were calculated by using eq 1 to provide the best fit for the experimental dipolar oscillation frequencies, and these are listed in Table 4. As seen in the table, the center phenyl ring has a value of 0.68 for the major order parameter. Each of the two side-wing phenyl rings has an order parameter of 0.50, which is considerably smaller than that for the center phenyl ring. These differences in the order parameters can be attributed to the differences in the orientations of the local ordering axes of the phenyl rings. The large magnitude of the order parameter of the center phenyl ring indicates that the molecule orients along the z axis of the center phenyl ring as observed in earlier studies.^{15–19} Hence, the director frame (x, y, z) is taken to coincide with that of the center phenyl ring (vide Figure 6A) with an order parameter of $S \approx S_{zz}$. The orientation β of the para-axes of the phenyl ring with respect to the orienting axis can then be obtained by using $S'_{zz}(II) \approx S * P_2(\cos \beta)$.³⁵ Accordingly, the angle β is found to be 24.9° between the phenyl ring-II and the center phenyl ring. Thus, the bent-angle between the side-wings of PMBAPH in B₁ mesophase is 130.3°, and the value typically matches with banana mesogens reported in the literature.^{14–17}

¹³C NMR Studies of BDBPTD in Smectic C Phase. *1D NMR in Smectic C Phase.* ¹³C NMR spectra of BDBPTD were recorded in the smectic C phase. The measurements in the nematic phase could not be performed in view of the high clearing temperature of the mesogen and the limitation of the NMR probe. The spectrum recorded at 210 °C in the smectic C mesophase is shown in Figure 4A. It shows nine peaks in the range of 140–229 ppm accounting for the core unit carbons and four peaks for terminal dodecyloxy chains (9–61 ppm). The peak at 153 ppm with high intensity indicates overlapping of many methine carbons. By making use of 2D spectral data, the assignment of carbon chemical shifts is made (Table 3). For the terminal dodecyloxy chain, the OCH₂ at 60.4 ppm and the methyl at 9.8 ppm are distinctly seen. The thiophene unit is expected to show one methine and one quaternary carbon peak in the static spectrum, which, however, could not be identified in the spectrum due to overlap with phenyl ring methine carbons. Spectra were also recorded at other temperatures in the range of 190–250 °C. Similar to the banana mesogen, the

chemical shifts of the methine carbons across this temperature range showed a very marginal variation of 1 ppm, suggesting that the mesogen maintains more or less the same orientational order in the temperature range investigated.

2D NMR of BDBPTD in Smectic C Phase. The 2D NMR spectrum of the mesogen recorded in the smectic C at 210 °C is shown in Figure 7. The spectrum reflects generally the

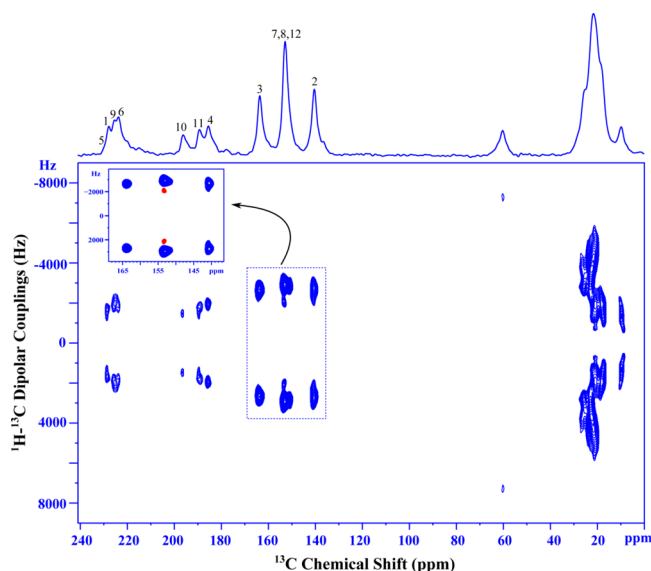
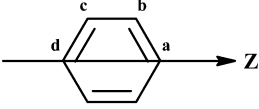


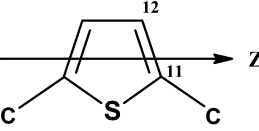
Figure 7. 2D SLF NMR spectrum of BDBPTD in smectic C phase at 210 °C. Red contour in the inset denotes thiophene ring methine carbon.

pattern observed in the 1D spectrum. However, a close examination reveals three contours around 153 ppm, which in the 1D spectrum showed a single peak. Two of these with a dipolar coupling of around 3 kHz are assigned to methine carbons of ring-II, while the third with a smaller dipolar coupling of 2.1 kHz is assigned to the CH carbon of the central thiophene ring (inset of Figure 7). Couplings of core unit quaternary carbons are found to be in the range of 1.5–1.8 kHz. All the dipolar couplings of the core unit carbons are listed

Table 5. Orientational Order Parameter Values of BDBPTD



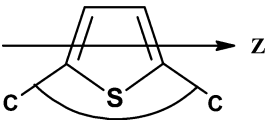
Side-Wing Phenyl Ring



Thiophene Ring

| ring | T (°C) | angles | | S' _{zz} | (S' _{xx} - S' _{yy}) | calculated dipolar oscillation frequencies (kHz) | | | | RMSD (kHz) |
|-----------|--------|------------|---------------|------------------|--|--|------|------|-------|------------|
| | | θ_b | θ_c | | | b | c | a | d | |
| I | 210.0 | 120.9 | 121.2 | 0.72 | 0.087 | 2.86 | 2.76 | 1.72 | 1.72 | 0.05 |
| II | 120.8 | 120.8 | 0.76 | 0.087 | 3.02 | 3.02 | 1.80 | 1.80 | 0.03 | |
| I | 230.0 | 120.6 | 121.0 | 0.68 | 0.075 | 2.75 | 2.62 | 1.60 | 1.61 | 0.05 |
| II | 120.3 | 120.4 | 0.70 | 0.075 | 2.91 | 2.88 | 1.63 | 1.63 | 0.04 | |
| | | T (°C) | θ_{12} | S _{zz} | (S _{xx} - S _{yy}) | 11 | | 12 | RMSD | |
| thiophene | | 210 | 126.1 | 0.85 | 0.212 | 1.61 | | 2.11 | 0.002 | |
| | | 230 | 125.8 | 0.82 | 0.173 | 1.50 | | 1.99 | 0.002 | |

Bent Angle



149.2° at 210 °C
143.6° at 230 °C

in Table 3. For the terminal chain, the OCH₂ and CH₃ contours are clearly seen from rest of the methylene carbons due to change in chemical shifts; in contrast to 1D spectrum, the 2D showed better separation of CH₂ carbons due to variation in ¹³C–¹H dipolar couplings.

The local order parameters of the side arm phenyl rings were calculated using the procedure outlined for earlier mesogen PMBAPH. In arriving at the order parameter values for a thiophene ring, a model of thiophene derived from the energy minimized structure obtained from DFT has been utilized, and the corresponding bond angles and bond-distances are used. For BDBPTD, the molecular frame is taken to coincide with the local thiophene axes, as shown in Figure 6B. The center thiophene ring order parameters were determined using eq 1 and using experimentally determined ¹³C–¹H dipolar couplings. Accordingly, at 210 °C, the thiophene order parameter is found to be 0.85, while for the side arm phenyl rings, the values are 0.76 and 0.72 for ring-II and ring-I, respectively (Table 5). By taking the ratios of side arm phenyl ring and thiophene order parameters, as done for PMBAPH, the bent angle is determined to be 149.2°.

A comparison of results of both the mesogens reveal interesting features. The remarkable feature of the 2D spectrum of BDBPTD in comparison to that of PMBAPH is the low ¹³C–¹H dipolar coupling value (~2 kHz) of thiophene methine carbon in contrast to the center phenyl ring methine carbons of PMBAPH (~10 kHz), though both have the bent-core structure. This is a consequence of the irregular pentagonal structure of thiophene as against the regular hexagonal structure of the phenyl ring and the corresponding difference in the angle of orientation of the C–H dipolar vector with respect to the local ordering axis. Again, the different geometry of thiophene, despite its aromatic nature, results in a significantly different bent angle for the two mesogens. Thus, for the benzene mesogen, the bent-angle is 130.3°, while it is 149.2° for the thiophene mesogen. The influence of variation in bent angle on the mesophase sequence is also clearly evident.

The benzene mesogen exhibits a B₁ phase, whereas thiophene mesogen shows only nematic and smectic C phases. Thus, the large bent-angle aids a calamitic mesophases, while the typical bent angles 120–130° favor the banana mesophases.²

In literature for many banana mesogens, the bent-angles have been determined from 1D chemical shifts in the mesophase.^{15,16} This method, on the one hand, requires identifying the overlapped resonances in the 1D NMR spectrum and assigning them to the individual carbons and on the other hand requires a knowledge of the chemical shift anisotropy (CSA) tensor values. It is well-known that the CSA tensors are very sensitive to neighboring environment, which is molecular structure specific. However, theoretical tools such as the DFT method are available, which can provide the required CSA information to a reasonable degree of accuracy. In contrast, as demonstrated in this study, the use of ¹³C–¹H dipolar couplings provides a simple and straightforward means of estimating the order parameter values. The ¹³C–¹H dipolar couplings show significant variations over the length of the molecule and exhibit features characteristic of the different structural features in the molecule. Thus, the central phenyl ring, the thiophene unit, the side arm phenyl rings all have characteristic dipolar coupling. As sufficient data on these systems is accumulated, it is expected that a visual examination of the spectrum will reveal the nature of the phase and the orientation of the different structural units. As the modern day design of liquid crystals moves away from the classical rodlike molecules, the 2D-NMR approach is likely to provide valuable information on the topology of the mesogenic molecule, which is one of the crucial parameters influencing the mesophase formation. It is to be noted that the banana molecules are difficult to align in magnetic field.^{18,19,42–44,49,50} However, if they align as noticed in this investigation, the ¹³C–¹H dipolar couplings provide significant insights.

CONCLUSION

Two bent-core mesogens based on benzene and thiophene with side-wing phenyl rings were investigated by solid state ^{13}C NMR spectroscopy. The benzene mesogen exhibited B_1 mesophase, while the thiophene mesogen showed dimorphism with nematic and smectic C phases. The ^{13}C NMR measurements were carried out in banana phase for benzene mesogen, whereas for the thiophene case, experiments were carried out in the smectic C mesophase. The ^{13}C – ^1H dipolar couplings were measured by 2D SLF spectroscopy. Some important observations were made from the 2D data of both the mesogens. The methine ^{13}C – ^1H dipolar couplings of center ring were found to be much higher (9.7–10.2 kHz) than the side wing rings (1.5–2.0 kHz). This was reflected on the orientational order values, which were found to be 0.68 and 0.50 for center as well as side-wing rings, respectively. Further, the ratios of order parameters of center as well as side wing rings resulted in a bent angle of 130.3° for benzene banana mesogen. For the thiophene case, the order parameter was 0.85 for the center ring, 0.72 and 0.76 for side wing phenyl rings, and the bent angle was 149.2° . The notable feature of the investigation was observation of high-order parameter for thiophene ring despite low ^{13}C – ^1H dipolar coupling (2.11 kHz) in contrast to the center ring of benzene mesogen (9.7–10.2 kHz), which was solely attributed to the geometry of the center ring. The appearance of the B_1 phase for benzene mesogen and nematic and smectic C phases for thiophene mesogen was a consequence of dissimilar bent angles, in spite of a bent-core structure for both compounds.

ASSOCIATED CONTENT

Supporting Information

Synthetic details, table of transition temperatures and enthalpy values of PMBAPH and BDBPTD, synthetic strategy schemes for target mesogens, figure of SAMPI-4 pulse sequence, DSC plot, and HOPM pictures. This material is available free of charge via the Internet at <http://pubs.acs.org>.

AUTHOR INFORMATION

Corresponding Author

*E-mail: kvr@sif.iisc.ernet.in.

Notes

The authors declare no competing financial interest.

ACKNOWLEDGMENTS

M.K.R. would like to express sincere thanks to Prof. K. Subramanyam Reddy, S. V. University, Tirupati, India, and Dr. A. B. Mandal, Director, CLRI, Chennai, India, for their help, constant support, and encouragement. The authors are thankful to Dr. R. Amaranatha Reddy, Sr. Research Chemist at PPG Industries Inc, United States, for technical discussions. The authors are also thankful to Dr. V. Subramanian, CLRI, for the quantum chemical calculations. M.K.R. and T.N.S. are grateful to Prof. V. A. Raghunathan and Ms. K. N. Vasudha, RRI, Bangalore, India, for the X-ray measurements. The authors are also thankful to Dr. S. Krishna Prasad, Centre for Soft Matter Research, Jalahalli, Bangalore 560013, India, for the help in interpretation of X-ray data. The use of the Bruker AV-III-400 and Bruker AV-III-500 NMR spectrometers funded by the Department of Science and Technology, New Delhi, at the NMR Research Centre, Indian Institute of Science, Bangalore, India, is gratefully acknowledged. T. Narasimhaswamy would

like to acknowledge the partial financial support from STRAIT project under XII five year plan of CSIR.

REFERENCES

- (1) Pelzl, B. G.; Diele, S.; Weissflog, W. Banana-Shaped Compounds-A New Field of Liquid Crystals. *Adv. Mater.* **1999**, *11*, 707–724.
- (2) Hird, M. Banana-shaped and other Bent-Core Liquid Crystals. *Liq. Cryst. Today* **2005**, *14*, 9–21.
- (3) Amaranatha Reddy, R.; Tschierske, C. Bent-Core Liquid Crystals: Polar Order, Superstructural Chirality and Spontaneous Desymmetrisation in Soft Matter Systems. *J. Mater. Chem.* **2006**, *16*, 907–961.
- (4) Takezoe, H.; Takanishi, Y. Bent-Core Liquid Crystals: Their Mysterious and Attractive World. *Jpn. J. Appl. Phys., Part 1* **2006**, *45*, 597–625.
- (5) Vaupotic, N.; Pociecha, D.; Gorecka, E. Polar and Apolar Columnar Phases Made of Bent-Core Mesogens. *Top. Curr. Chem.* **2012**, *318*, 218–302.
- (6) Eremin, A.; Jakli, A. Polar Bent-Shape Liquid Crystals-from Molecular Bend to Layer Splay and Chirality. *Soft Matter* **2013**, *9*, 615–637.
- (7) Ros, M. B.; Serrano, J. L.; Rosario de la Fuente, M.; Folcia, C. L. Banana-Shaped Liquid Crystals: A New Field to Explore. *J. Mater. Chem.* **2005**, *15*, 5093–5098.
- (8) Weissflog, W.; Nadasi, H.; Dunemann, U.; Pelzl, G.; Diele, S.; Eremin, A.; Kresse, H. Influence of Lateral Substituents on the Mesophase Behaviour of Banana-Shaped Mesogens. *J. Mater. Chem.* **2001**, *11*, 2748–2758.
- (9) Madsen, L. A.; Dingemans, T. J.; Nakata, M.; Samulski, E. T. Thermotropic Biaxial Nematic Liquid Crystals. *Phys. Rev. E* **2004**, *92*, 145505–145509.
- (10) Dingemans, T. J.; Madsen, L. A.; Zafiroopoulos, N. A.; Lin, W.; Samulski, E. T. Uniaxial and Biaxial Nematic Liquid Crystals. *Philos. Trans. R. Soc., A* **2006**, *364*, 2681–2696.
- (11) Francescangeli, O.; Samulski, E. T. Insights into the Cybotactic Nematic Phase of Bent-Core Molecules. *Soft Matter* **2010**, *6*, 2413–2420.
- (12) Vita, F.; Placentino, I. F.; Ferrero, C.; Singh, G.; Samulski, E. T.; Francescangeli, O. Electric Field Effect on the Phase Diagram of a Bent-Core Liquid Crystal. *Soft Matter* **2013**, *9*, 6475–6481.
- (13) Ananda Rama Krishnan, S.; Weissflog, W.; Friedemann, R. Quantum Chemical Studies on the Conformational Behaviour of Substituted Banana-Shaped Mesogens with a Central 1,3-Phenylene Unit. *Liq. Cryst.* **2005**, *32*, 847–856.
- (14) Eremin, A.; Nadasi, H.; Pelzl, G.; Diele, S.; Kresse, H.; Weissflog, W.; Grande, S. Paraelectric–Antiferroelectric Transitions in the Bent-Core Liquid-Crystalline Materials. *Phys. Chem. Chem. Phys.* **2004**, *6*, 1290–1298.
- (15) Weissflog, W.; Dunemann, U.; Schröder, M. W.; Diele, S.; Pelzl, G.; Kresse, H.; Grande, S. Field-Induced Inversion of Chirality in SmCP_A Phases of New Achiral Bent-Core Mesogens. *J. Mater. Chem.* **2005**, *15*, 939–946.
- (16) Wirth, I.; Diele, S.; Eremin, A.; Pelzl, G.; Grande, S.; Kovalenko, L.; Pancenko, N.; Weissflog, W. New Variants of Polymorphism in Banana-Shaped Mesogens with Cyano-Substituted Central Core. *J. Mater. Chem.* **2001**, *11*, 1642–1650.
- (17) Nádasi, H.; Weissflog, W.; Eremin, A.; Pelzl, G.; Diele, S.; Das, B.; Grande, S. Ferroelectric and Antiferroelectric “Banana Phases” of New Fluorinated Five-Ring Bent-Core Mesogens. *J. Mater. Chem.* **2002**, *12*, 1316–1324.
- (18) Xu, J.; Fodor-Csorba, K.; Dong, R. Y. Orientational Ordering of a Bent-Core Mesogen by Two-Dimensional ^{13}C NMR Spectroscopy. *J. Phys. Chem. A* **2005**, *109*, 1998–2005.
- (19) Dong, R. Y.; Fodor-Csorba, K.; Xu, J.; Domenici, V.; Prampolini, G.; Veracini, C. A. Deuterium and Carbon-13 NMR Study of a Banana Mesogen: Molecular Structure and Order. *J. Phys. Chem. B* **2004**, *108*, 7694–7701.
- (20) Becke, A. D. Density-Functional Thermochemistry. III. The Role of Exact Exchange. *J. Chem. Phys.* **1993**, *98*, 5648–5652.

- (21) Lee, C. T.; Yang, W. T.; Parr, R. G. Development of the Colle-Salvetti Correlation Energy Formula into a Functional of the Electron Density. *Phys. Rev. B* **1988**, *37*, 785–789.
- (22) Ditchfield, R. Molecular Orbital Theory of Magnetic Shielding and Magnetic Susceptibility. *J. Chem. Phys.* **1972**, *56*, 5688–5691.
- (23) Cheeseman, J. R.; Trucks, G. W.; Keith, T. A.; Frisch, M. J. A Comparison of Models for Calculating Nuclear Magnetic Resonance Shielding Tensors. *J. Chem. Phys.* **1996**, *104*, 5497–5509.
- (24) Aliev, A. E.; Murias, D. C.; Zhou, S. Scaling Factors for Carbon NMR Chemical Shifts Obtained from DFT B3LYP Calculations. *J. Mol. Struct.: THEOCHEM* **2009**, *893*, 1–5.
- (25) Frisch, M. J.; Trucks, G. W.; Schlegel, H. B.; Scuseria, G. E.; Robb, M. A.; Cheeseman, J. R.; Scalmani, G.; Barone, V.; Mennucci, B.; Petersson, G. A.; et al. GAUSSIAN 09, revision A.02; Gaussian, Inc.: Wallingford, CT, 2009.
- (26) Gupta, S. K.; Setia, N.; Sidiq, S.; Gupta, M.; Kumar, S.; Pal, S. K. New Perylene-Based Non-Conventional Discotic Liquid Crystals. *RSC Adv.* **2013**, *3*, 12060–12065.
- (27) Fung, B. M.; Khitritin, A. K.; Ermolaev, K. An Improved Broad Band Decoupling Sequence for Liquid Crystals and Solids. *J. Magn. Reson.* **2000**, *142*, 97–101.
- (28) Nevzorov, A. A.; Opella, S. J. Selective Averaging for High-Resolution Solid-State NMR Spectroscopy of Aligned Samples. *J. Magn. Reson.* **2007**, *185*, 59–70.
- (29) Kesava Reddy, M.; Subramanyam Reddy, K.; Yoga, K.; Prakash, M.; Narasimhaswamy, T.; Mandal, A. B.; Lobo, N. P.; Ramanathan, K. V.; Shankar Rao, D. S.; Krishna Prasad, S. Structural Characterization and Molecular Order of rodlike Mesogens with Three- and Four-Ring Core by XRD and ^{13}C NMR Spectroscopy. *J. Phys. Chem. B* **2013**, *117*, 5718–5729.
- (30) Das, B. B.; Ajitkumar, T. G.; Ramanathan, K. V. Improved Pulse Schemes for Separated Local Field Spectroscopy for Static and Spinning Samples. *Solid State Nucl. Magn. Reson.* **2008**, *33*, 57–63.
- (31) Kesava Reddy, M.; Subramanyam Reddy, K.; Narasimhaswamy, T.; Das, B. B.; Lobo, N. P.; Ramanathan, K. V. ^{13}C – ^1H Dipolar Couplings for Probing Rod-Like Hydrogen Bonded Mesogens. *New J. Chem.* **2013**, *37*, 3195–3206.
- (32) Bedel, J. P.; Rouillon, J. C.; Marcerou, J. P.; Laguerre, M.; Achard, M. F.; Nguyen, H. T. Physical Characterization of B₁ and B₂ Phases in a Newly Synthesized Series of Banana Shaped Molecules. *Liq. Cryst.* **2000**, *27*, 103–113.
- (33) Dierking, I. *Textures of Liquid Crystals*; Wiley-VCH: Weinheim, Germany, 2003.
- (34) Manohara, C.; Kelkara, V. K.; Yakhmia, J. V. Smectic C to Nematic Transition in p-n-Heptyloxybenzylidene-p-aminobenzoic Acid. *Mol. Cryst. Liq. Cryst.* **1978**, *48*, 165–174.
- (35) Deniz, K. U.; Paranjpe, A. S.; Mirza, E. B.; Parvathanathan, P. S.; Patel, K. S. DSC and X-Ray Diffraction Investigations of Phase Transitions in HxBABA and NBABA. *Le Journal de Physique Colloques* **1979**, *C3*, 136–140.
- (36) Fung, B. M. ^{13}C NMR Studies of Liquid Crystals. *Prog. Nucl. Magn. Reson. Spectrosc.* **2002**, *41*, 171–186.
- (37) Narasimhaswamy, T. Solid-State ^{13}C NMR Spectroscopy: A Powerful Characterization tool for Thermotropic Liquid Crystals. *J. Indian. Inst. Sci.* **2010**, *90*, 37–53.
- (38) Dong, R. Y. *Nuclear Magnetic Resonance Spectroscopy of Liquid Crystals*; World Scientific: Singapore, 2010.
- (39) Ramamoorthy, A., Ed. *Thermotropic Liquid Crystals: Recent Advances*; Springer: Dordrecht, Netherlands, 2007.
- (40) Lobo, N. P.; Prakash, M.; Narasimhaswamy, T.; Ramanathan, K. V. Determination of ^{13}C Chemical Shift Anisotropy Tensors and Molecular Order of 4-Hexyloxybenzoic Acid. *J. Phys. Chem. A* **2012**, *116*, 7508–7515.
- (41) Kalaivani, S.; Narasimhaswamy, T.; Das, B. B.; Lobo, N. P.; Ramanathan, K. V. Phase Characterization and Study of Molecular Order of a Three-Ring Mesogen by ^{13}C NMR in Smectic C and Nematic Phases. *J. Phys. Chem. B* **2011**, *115*, 11554–11565.
- (42) Domenici, V.; Veracini, C. A.; Zalar, B. How Do Banana-Shaped Molecules get Oriented (if they do) in the Magnetic Field? *Soft Matter* **2005**, *1*, 408–411.
- (43) Domenici, V. Dynamics in the Isotropic and Nematic Phases of Bent-Core Liquid Crystals: NMR Perspectives. *Soft Matter* **2011**, *7*, 1589–1598.
- (44) Domenici, V.; Veracini, C. A.; Fodor-Csorba, K.; Prampolini, G.; Cacelli, I.; Lebar, A.; Zalar, B. Banana-Shaped Molecules Peculiarly Oriented in a Magnetic Field: ^2H NMR Spectroscopy and Quantum Mechanical Calculations. *ChemPhysChem* **2007**, *8*, 2321–2330.
- (45) Fung, B. M. Liquid Crystalline Samples: Carbon-13 NMR. *Encycl. Nucl. Magn. Reson.* **1996**, *4*, 2744–2751.
- (46) Nagaraja, C. S.; Ramanathan, K. V. Determination of Order Parameters of Liquid Crystals: Use of Dipolar Oscillations Enhanced by Lee-Goldburg Decoupling. *Liq. Cryst.* **1999**, *26*, 17–21.
- (47) Gan, Z. Spin Dynamics of Polarization Inversion Spin Exchange at the Magic Angle in Multiple Spin Systems. *J. Magn. Reson.* **2000**, *143*, 136–143.
- (48) Fung, B. M.; Afzal, J.; Foss, T. L.; Chau, M.-H. Nematic Ordering of 4-n-Alkyl-4'-Cyanobiphenyls Studied by Carbon-13 NMR with Off-Magic-Angle Spinning. *J. Chem. Phys.* **1986**, *85*, 4808–4814.
- (49) Dong, R. Y. A Comparative ^{13}C NMR Study of Local Ordering in a Homologous Series of Bent-Core Liquid Crystals. *J. Phys. Chem. B* **2009**, *113*, 1933–1939.
- (50) Xu, J.; Dong, R. Y.; Domenici, V.; Fodor-Csorba, K.; Veracini, C. A. ^{13}C and ^2H NMR Study of Structure and Dynamics in Banana B₂ Phase of a Bent-Core Mesogen. *J. Phys. Chem. B* **2006**, *110*, 9434–9441.